

RESEARCH

Open Access



Intrauterine growth restriction, defined by an elevated brain-to-liver weight ratio, affects faecal microbiota composition and, to a lesser extent, plasma metabolome profile at different ages in pigs

Roberta Ruggeri^{1,2}, Giuseppe Bee^{1*}, Federico Correa², Paolo Trevisi² and Catherine Ollagnier¹

Abstract

Background Intrauterine growth restriction (IUGR) affects up to 30% of piglets in a litter. Piglets exposed to IUGR prioritize brain development during gestation, resulting in a higher brain-to-liver weight ratio (BrW/LW) at birth. IUGR is associated with increased mortality, compromised metabolism, and gut health. However, the dynamic metabolic and microbial shifts in IUGR-affected pigs remain poorly understood. This study aimed to investigate the longitudinal effects of IUGR, defined by a high BrW/LW, on the composition of faecal microbiota and plasma metabolome in pigs from birth to slaughter. One day (± 1) after birth, computed tomography was performed on each piglet to assess their brain and liver weights. The pigs with the highest (IUGR = 12) and the lowest (NORM = 12) BrW/LW were selected to collect faeces and blood during lactation (day 16 ± 0.6 , T1) and at the end of the starter period (day 63 ± 8.6 , T2) and faeces at the beginning (day 119 ± 11.4 , T3) and end of the finisher period (day 162 ± 14.3 , T4).

Results Faecal microbial Alpha diversity remained unaffected by IUGR across all time points. However, the Beta diversity was influenced by IUGR at T1 ($P=0.002$), T2 ($P=0.08$), and T3 ($P=0.03$). Specifically, IUGR pigs displayed higher abundances of *Clostridium sensu stricto 1* ($P_{\text{adj}}=0.03$) and *Romboutsia* ($P_{\text{adj}}=0.05$) at T1, *Prevotellaceae NK3B31 group* ($P_{\text{adj}}=0.02$), *Rikenellaceae RC9 gut group* ($P_{\text{adj}}=0.03$), and *Alloprevotella* ($P_{\text{adj}}=0.03$) at T2, and *p-2534-18B5 gut group* ($P_{\text{adj}}=0.03$) at T3. Conversely, the NORM group exhibited higher abundances of *Ruminococcus* ($P_{\text{adj}}=0.01$) at T1, HT002 ($P_{\text{adj}}=0.05$) at T2, and *Prevotella_9* ($P_{\text{adj}} < 0.001$) at T3. None of the plasma metabolites showed significant differences at T1 between the IUGR and NORM pigs. However, at T2, asparagine was lower in the IUGR compared to the NORM group ($P < 0.05$).

Conclusions These findings show that growth restriction in the uterus has a significant impact on the faecal microbiota composition in pigs, from birth to the beginning of the finisher period, but minimally affects the plasma metabolome profile.

Keywords Asparagine, Beta diversity, Computed tomography, Intrauterine growth restriction, Faecal microbiota, Metabolites

*Correspondence:

Giuseppe Bee

giuseppe.bee@agroscope.admin.ch

Full list of author information is available at the end of the article



© The Author(s) 2025. **Open Access** This article is licensed under a Creative Commons Attribution-NonCommercial-NoDerivatives 4.0 International License, which permits any non-commercial use, sharing, distribution and reproduction in any medium or format, as long as you give appropriate credit to the original author(s) and the source, provide a link to the Creative Commons licence, and indicate if you modified the licensed material. You do not have permission under this licence to share adapted material derived from this article or parts of it. The images or other third party material in this article are included in the article's Creative Commons licence, unless indicated otherwise in a credit line to the material. If material is not included in the article's Creative Commons licence and your intended use is not permitted by statutory regulation or exceeds the permitted use, you will need to obtain permission directly from the copyright holder. To view a copy of this licence, visit <http://creativecommons.org/licenses/by-nc-nd/4.0/>.

Background

Intrauterine growth restriction (IUGR) is characterised by the failure of the foetus to achieve its genetic growth potential during gestation [1]. As a consequence of genetic selection to improve litter size, this condition affects up to 20–30% of newborn piglets in the modern pig industry [2, 3]. IUGR is associated with an increased risk of neonatal morbidity and mortality, as well as with long-term effects resulting from foetal programming, such as impaired metabolism [4], stunted postnatal growth, and reduced feed conversion efficiency [5, 6]. For these reasons, IUGR poses a significant problem within the pig production system, negatively affecting overall production efficiency [5].

Numerous studies have demonstrated a strong relationship between the health and growth of pigs and the optimal functioning of their gastrointestinal tract (GIT) [2]. The gastrointestinal tract (GIT), particularly the small intestine, is crucial for the digestion, absorption, and transportation of nutrients, water, and electrolytes. It also acts as a defensive barrier against pathogens, dietary toxins, and antigens [7]. The GIT hosts a dynamic microbiota, including bacteria, viruses, archaea, and fungi. This microbial population regulates the development and function of the immune system, limits the nutrients available to potential pathogens to grow [8], and is involved in the host's carbohydrate, amino acid, and lipid metabolism [9].

Growing evidence suggests that the uterine environment can influence intestinal development, potentially compromising both its function and microbial colonisation [2, 10]. Several studies have shown reduced intestinal length and weight, decreased villus height, and increased crypt depth, as well as changes in the proteomic profile in IUGR-affected piglets compared to their normal littermates from the lactation period [11–14] up to 70 days of age [2]. IUGR affects not only the structure but also the microbial colonisation of the GIT. According to Zhang et al. [10], newborn piglets exposed to growth restriction during foetal development exhibited reduced microbial diversity and a distinct taxonomic profile compared to their normal littermates.

Clear differences between IUGR and normal neonates were also demonstrated at the blood metabolome level in both human and pig studies [11, 15]. Although data on blood metabolomic profiling in IUGR are limited, the metabolic changes identified in IUGR neonates seem to indicate an early pattern of glucose intolerance, insulin resistance, alterations in lipogenesis and lipid oxidation, energy, and amino acid metabolism [11, 15, 16]. IUGR leads to a reduced glucose supply during foetal development. In response, the foetus initiates metabolic and endocrine adaptations to optimise the utilisation of

alternative energy sources, such as fatty acids. Indeed, within these adaptive responses, an increase in adipocyte proliferation has been reported in IUGR foetuses [17–19]. The increased adipogenesis facilitates the long-term storage of fatty acids, which can, in turn, undergo oxidation to provide energy for the organism. This adaptation is crucial for enhancing the foetus's survival under conditions of intermittent or poor nutrition [17, 19]. Moreover, different studies have suggested that this increased adipogenesis continues in postnatal life in IUGR-affected pigs [19, 20].

Considering the modifications that IUGR imposes on the structure and function of the intestinal mucosa, along with the endocrine and metabolic mechanisms established during gestation in response to nutrient restriction, we expected distinct differences in the faecal microbiota and blood metabolome profiles between IUGR and normal piglets. Specifically, we hypothesised a reduction in microbial diversity and shifts in the abundances of bacterial taxa involved in nutrient digestion, inflammatory responses, and susceptibility to diseases, such as *Ruminococcus*, *Lactobacillus*, *Prevotella*, *Escherichia-Shigella*, and *Pasteurella*, in IUGR compared to normal pigs. Moreover, we hypothesised changes in the concentration of metabolites involved in lipid metabolism, such as increased plasma glycerol and ketone bodies, reflecting an increased reliance on fat metabolism for energy supply in the IUGR group, particularly during the early stages of life, as well as alterations in energy and amino acid metabolism, including lower levels of plasma glucose and essential amino acids in IUGR compared to normal pigs.

To test these hypotheses, computed tomography (CT) scan imaging was used in this study to non-invasively assess the brain-to-liver weight ratio (BrW/LW) in newborn piglets, enabling an accurate diagnosis of IUGR [21]. In addition, blood and faeces samples were obtained from both IUGR and normal pigs at different ages to determine the effects of IUGR on faecal microbiota and plasma metabolome.

Methods

This experiment was approved (experimental approval number 32751_FB) by the ethics committee of the canton of Fribourg (Switzerland).

Animal selection and classification

This research was carried out at the Agroscope swine research facility in Posieux, Switzerland. Detailed information on all the procedures concerning the CT scan and the determination of the brain and liver weight is described in detail by Ruggeri et al. [21]. Briefly, the study included 268 piglets of the Swiss Large White

breed (134 females and 134 males) born from 26 litters that were obtained from two farrowing batches (14 litters in the first batch and 12 litters in the second batch). On day 1 (± 1) after birth, CT scan imaging was performed on all piglets to determine the volume of the brain and liver and subsequently calculate their weight. All the pigs were sampled for blood and faeces during lactation (day 16 ± 0.6 [mean \pm SD], T1), and at the end of the starter period (day 63 ± 8.6 , T2), and for faeces at the beginning (day 119 ± 11.4 , T3) and end of the finisher period (day 162 ± 14.3 , T4). For the analyses of faecal microbiota and plasma metabolome, we retrospectively selected samples collected at T1 from two groups: the 12 IUGR piglets (birth weight: 1.1 ± 0.19) with the highest BrW/LW ratio (1.00 ± 0.09), and the 12 NORM piglets (birth weight: 1.8 ± 0.29) with the lowest BrW/LW ratio (0.36 ± 0.04). One piglet (NORM=1) died before weaning, and the others ($n=23$, IUGR=12, NORM=11) were weaned at 25 ± 1.5 days of age. At T2, only 15 out of the initial 24 pigs, from which blood and faeces samples were selected at T1, remained available. To ensure the intended group sizes of 12 IUGR and 12 NORM pigs for subsequent analyses, 3 samples of IUGR and 6 samples of NORM pigs were replaced with 3 samples of IUGR pigs and 6 samples of NORM pigs with a comparable BrW/LW ratio (IUGR: 0.90 ± 0.05 , birth weight: 1.1 ± 0.12 ; NORM: 0.43 ± 0.04 , birth weight: 1.9 ± 0.12) as detailed in Supplementary Table 1 and Additional File 1.

The data on average daily gain (ADG), average daily feed intake (ADFI), gain-to-feed ratio, and body composition for the 24 selected pigs were previously analysed as part of a larger population study [21].

Rearing conditions and feeding

The conditions in which the pigs were reared and the feeding techniques employed were described by Ruggeri et al. [21]. Briefly, the pigs were raised under a conventional Swiss rearing system with unrestricted access to water and straw provided in the pens throughout the entire experimental period.

The piglets had ad libitum access to the same standard pre-/early postweaning diet from day 16 after birth until approximately 14 days post-weaning. Later, they were provided unrestricted access to the same starter, grower, and finisher diets. The transition from the starter to the grower diet and from the grower to the finisher diet occurred when the pigs' body weight (BW) was ≥ 20 kg and ≥ 60 kg, respectively, on the day of weekly weighing.

During the grower-finisher period, automatic feeders and an individual pig recognition system were employed to monitor daily feed intake as described by Ruggeri et al. [21]. Starting from week 2 after birth, the selected pigs were weighed individually once a week until slaughter.

The ADG was calculated for the lactation, starter, grower, and finisher periods. In addition, feed intake was monitored from 20 kg until slaughter, and the gain-to-feed ratio was computed for each individual pig.

Body composition determined by dual X-ray absorptiometry

A GE lunar dual-energy X-ray absorptiometry (DXA; i-DXA, GE Healthcare Switzerland, Glattbrugg, Switzerland) device equipped with a narrow-angle fan beam (Collimator Model 42,129) was employed to scan the selected pigs at weaning (IUGR=12, NORM=11), at the start of the grower period (IUGR=12, NORM=12) and at the end of the finisher period (IUGR=11, NORM=11). The detailed procedures for pig handling and DXA scan image analysis have been described by Kasper et al. [22]. Briefly, on the day of the scan, pigs were anesthetized with isoflurane and scanned in sternal recumbency. The entire body scan in thick mode was selected for analysis. Processed images were refined to eliminate artifacts and position regions of interest. Output variables from DXA, including body mass, lean mass, fat mass, bone mineral content, and bone mineral density, were exported from the enCORE software and evaluated at weaning, the beginning of the grower period, and at the end of the finisher period.

Faeces sampling

Faeces (~ 2 g) were collected from the piglets (IUGR=12, NORM=12) directly from the rectum just before the administration of the pre-/early postweaning diet (T1). Similarly, faeces were collected from the pigs (IUGR=12, NORM=12) at the end of the starter period (T2), at the beginning of the finisher period (T3), and at the end of the finisher period (T4). After collection, each sample was divided into two aliquots, snap-frozen in liquid nitrogen, and stored at -80°C .

Microbial DNA extraction, amplification, and sequencing

Total bacterial DNA for microbiota analysis was extracted from the faecal samples using the FastDNA Spin Kit for Soil (MP Biomedicals, Europe, LLC) according to the manufacturer's instructions. DNA quantity and quality were assessed with a Nanodrop ND 1000 spectrophotometer (Nanodrop Technologies Inc., Wilmington, DE, USA). The DNA was amplified, specifically targeting the V3–V4 hypervariable regions of the 16S rRNA gene. Amplicons were produced using the primers Pro341F: 50-TCGTCCGGCAGCGTCAGATGTGTAT AAGAGACAGCCTACGGGNBGCASCAG-30 and Pro805R: 50GTCTCGTGGGCTCGGAGATGTGTATAA GAGACAGGACTACNVGGGTATCTAATCC-30 [23], using Platinum TM Taq DNA Polymerase High Fidelity

(Thermo Fisher Scientific, Italy). The libraries were prepared according to the standard protocol for MiSeq Reagent Kit v3 and underwent sequencing on the MiSeq platform (Illumina Inc., San Diego, CA, USA).

Blood sampling

Blood (~ 3 mL) was collected from the piglets (IUGR = 12, NORM = 12) via the jugular vein using heparin-treated tubes at T1 and T2. The samples were refrigerated on ice after collection for 30 min. Plasma was then separated from the whole blood through centrifugation at 3000 rpm for 10 min. Following centrifugation, each plasma sample was split into two aliquots and stored at -80 °C until metabolome analysis via proton nuclear magnetic resonance (¹H-NMR).

Plasma ¹H-NMR analysis

An ¹H-NMR analysis solution with D₂O, 10 mmol/L of 3-(trimethylsilyl)-propionic-2,2,3,3-d₄ acid sodium salt, and 2 mmol/L of NaN₃ was prepared. The pH of the solution was set at 7.00 ± 0.02 using phosphate buffer 1 M. The acid sodium salt was employed as a reference for the NMR chemical shift. To avoid microorganism proliferation, NaN₃ was used. Before the ¹H-NMR analysis, 1 mL of each plasma sample was centrifuged (18,630 g; 900 s; 4 °C). Then, 0.7 mL of supernatant was added to 0.1 mL of the ¹H-NMR solution. Finally, centrifugation was performed on each sample once again, as previously described. ¹H-NMR spectra were registered (600.13 MHz; 298 K) with an AVANCE™ III spectrometer (Bruker, Milan, Italy), provided with Topspin v3.5 software. Signals from broad resonances due to large molecules were suppressed with a CPMG filter. The CPMG filter was composed of 400 echoes with a τ of 400 μs and a 180° pulse of 24 μs, for a total filter of 330 ms. The water residual signal was suppressed using presaturation, employing the cpmgpr1d sequence included in the standard pulse sequence library.

Each spectrum was generated by combining 256 transients, each consisting of 32,000 data points covering a frequency window of 7184 Hz, with intervals separated by a relaxation delay of 5 s. ¹H-NMR spectra were then phase-adjusted in Topspin v3.5 and exported to ASCII format employing the built-in script convbin2asc. Spectra were processed with R software [24] using in-house developed scripts. Baseline adjustment on spectra was performed by differentiating baseline imperfection from NMR signals according to the “rolling ball” principle [25], as implemented in the R package baseline [26].

Signal assignment was performed by comparing their chemical shift and multiplicity with the Human Metabolome Database [27] and the Chenomx software library (Chenomx Inc., Edmonton, Canada, v10). Plasma

molecule concentrations were assessed by quantifying the molecules of the first sample analysed using an external standard. Variations in water content among samples were adjusted using probabilistic quotient normalization [28]. The quantification of each metabolite was assessed using rectangular integration, considering one of its signals was free from interference [29].

Statistical analysis and bioinformatic analysis of microbiome data

All calculations and statistical analyses were performed using Python programming language (version 3.8.8) and R (version 4.0.2). The data on ADG, feed intake, and body composition were analysed in R with linear mixed-effect models using the “lmer” function of the lme4 package. The category (IUGR, NORM) and sex (female, castrate) were considered fixed effects, and the litter of origin was considered a random effect. The two-way interaction between the two fixed effects was consistently assessed and removed if not significant. The pig was considered the experimental unit. Analysis of data regarding ADG was conducted individually for the lactation, starter, grower, and finisher periods. Data on feed intake were analysed separately for the grower and finisher periods. Analysis of body composition data was conducted separately at weaning, the beginning of the grower period, and the end of the finisher period.

Microbiota analysis was carried out in R using the DADA2 pipeline [30], and taxonomic categories were assigned using the Silva Database (release 138.1) as a reference for the assignment [31]. Alpha (Shannon, Chao1, and Simpson indices) and Beta diversity (calculated as Bray Curtis distance matrix), as well as the abundances of taxonomic categories, were calculated and analysed with R software 3.6, using the PhyloSeq [32], Vegan [33], and microbiomeMarker [34] packages. Differences between groups regarding Alpha diversity indices were tested using a linear mixed model that included category (IUGR, NORM), time (T1, T2, T3, T4), and their interaction as fixed factors, with the litter of origin considered as a random factor. Then, a separate model within each time point was performed including only the category as a fixed factor and the litter of origin as a random factor. For Beta diversity, a dissimilarity matrix was constructed using the Bray–Curtis distance matrix as metrics, and the results were plotted using a non-metric multidimensional scaling (NMDS) plot. Furthermore, the betadisper test was conducted to test differences in the samples' dispersion among the groups. Differences were tested using a PERMANOVA (Adonis) model with 9,999 permutations, including category, time, and their interaction, and litter of origin as factors. A second PERMANOVA model was then performed within each time point, including the

category as a factor. For the differential analysis of taxa, the LEfSe algorithm was used at the genus level. Specifically, taxa were considered significant if they possessed a Linear Discriminant Analysis (LDA) score >4 and a $P_{\text{adj}} < 0.05$ within each time point, including the category as a factor.

For the metabolome data, all calculations and statistical analyses were performed using Python. The Shapiro–Wilk test was performed to identify the metabolites whose concentrations in the plasma showed a normal distribution, and Student's *t*-test was used to compare their concentrations in plasma samples for the IUGR and NORM groups. Metabolites whose concentrations did not show a normal distribution were compared between the two groups using the non-parametric Mann–Whitney test. The Benjamini–Hochberg correction was applied in both cases to account for the risk of inflation associated with multiple comparisons. Before being subjected to unsupervised and supervised algorithms, the concentration of each metabolite was normalised and centred. Principal component analysis (PCA) and orthogonal projection to latent structures-discriminant analysis (OPLS-DA) were employed as unsupervised and supervised methods in the multivariate analysis, respectively. PCA was used for the identification of outliers (Mahalanobis distance metric) as well as the spontaneous clustering of similar samples in the scatter plot of the two principal components. In the OPLS-DA analysis, the X matrix consisted of metabolite concentrations, while the Y vector contained information regarding the group (IUGR or NORM). The goodness of fit of the OPLS-DA model (R²_Y) was reported, and predictive performance was assessed through cross-validation. Metrics such as the predictive ability of the model (Q²_Y) and the predictive ability of permuted models (Q²_Y-perm) were calculated for evaluation. OPLS-DA loading plots were used to illustrate the metabolites that contributed the most to the separation between the IUGR and NORM groups. The identification of metabolites of interest was made through the combination of the variable importance in the projection (VIP) and the loading between the metabolite in the X matrix and the predictive latent variable (pLV) of the model. Metabolites with VIP > 1.0 and absolute high loading values were considered important in the metabolomics signature [35].

Correlation analyses between microbiota and metabolome data were performed using Python. Only metabolites within the quantifiable range for each sample and bacterial genera with an average relative abundance above 0.05% were included (bacterial genera with a relative abundance of zero in most samples were excluded from the analyses). The Shapiro–Wilk test was used to assess the normality of the metabolite and bacterial genera

distributions. For pairs where both variables followed a normal distribution, Pearson's correlation coefficient was employed. Otherwise, Spearman's correlation was used. To account for the risk of false positives associated with multiple comparisons, the Benjamini–Hochberg correction was applied. Correlations with a coefficient (r) > 0.6 and a Benjamini–Hochberg adjusted p -value < 0.05 were considered significant. A global analysis was first conducted across all samples, followed by a targeted analysis focusing on metabolites and bacterial genera that exhibited significant differences between IUGR and NORM pigs.

Results

Average daily gain from birth to slaughter

Throughout the lactation period, IUGR piglets exhibited slower growth rates compared to their NORM littermates (Table 1). The ADG of IUGR females was 0.16 kg/d lower ($P < 0.01$) than their NORM counterparts. Similarly, IUGR castrated piglets grew 0.09 kg/d ($P = 0.06$) slower than the NORM castrates. From weaning to the end of the starter period, IUGR pigs displayed a 0.08 kg/d lower ($P < 0.01$) ADG than the NORM group (Table 1). Likewise, in the grower period, IUGR pigs grew slower than NORM pigs, as their ADG was 0.13 kg/d lower ($P = 0.01$), despite similar average daily feed intake (Table 2). In the finisher period, IUGR status did not affect the growth rates in terms of ADG (Table 1) nor the average daily feed intake (Table 2). The BW at slaughter was comparable between the two groups, although IUGR pigs were 18 days older ($P < 0.01$) than NORM pigs. In addition, IUGR pigs exhibited lower feed efficiency compared to their NORM counterparts in both the grower ($P = 0.01$) and finisher periods ($P = 0.02$, Table 2).

Body composition determined by dual X-ray absorptiometry

Regardless of sex, the proportions of bone, lean mass, and fat mass in relation to body mass were unaffected by the IUGR status at weaning. The only notable difference between the two groups was observed in bone mineral density, which was higher ($P = 0.03$) in IUGR pigs compared to their NORM counterparts (Table 3). Similarly, the percentages of lean and fat mass in the body were similar between IUGR and NORM pigs at the end of the starter period. However, the proportions of bone ($P < 0.001$) and bone mineral density ($P = 0.02$) in relation to body mass were lower in IUGR compared to NORM pigs at the end of the starter period (Table 3). In the finisher period, there were no differences between IUGR and NORM castrates, nor between IUGR and NORM females (Table 3).

Table 1 Average daily gain during lactation, starter, grower, and finisher periods

Item ³	Category ¹				SEM ⁴	P-value ²		
	IUGR	NORM	females	castrates		Category	Sex	Category*Sex
Lactation ⁵	0.14	0.26	0.21	0.19	0.015	< 0.01	0.30	< 0.01 ⁶
Starter	0.34	0.42	0.38	0.38	0.022	< 0.01	0.70	0.29
Grower	0.80	0.93	0.83	0.90	0.034	0.01	0.05	0.34
Finisher	0.92	0.97	0.90	0.99	0.027	0.24	< 0.001	0.65

Effect of classifying the pigs based on the brain-to-liver weight ratio (BrW/LW) at birth and sex on average daily gain (ADG, kg/d) from birth to slaughter

¹ Category = IUGR: piglets with the highest brain-to-liver weight ratio (BrW/LW); NORM: piglets with the lowest BrW/LW

² P-value for the main effect of the category, sex, and their interaction

³ ADG = average daily gain

⁴ Pooled SEM

⁵ One piglet (NORM = 1) died during the lactation period (IUGR = 12, NORM = 11)

⁶ Significant interaction between category and sex: IUGR females ($n = 8$): 0.13^a kg/d; NORM females ($n = 7$): 0.29^{bc} kg/d; IUGR castrates ($n = 4$): 0.15^{ac} kg/d; NORM castrates ($n = 4$): 0.24^c kg/d. Different letters (a, b, c) indicate statistically significant ($P < 0.05$) differences between groups

Table 2 Growth performance traits in the grower and finisher periods

Item ⁴	Category ¹		Sex		SEM ³	P-value ²		
	IUGR	NORM	females	castrates		Category	Sex	Category × Sex
Number of pigs	12	12	12	12				
<i>Body weight at the start of,</i> kg								
Grower period	25.4	26.8	26.5	25.6	1.77	0.36	0.19	0.07
Finisher period	62.9	63.4	63.2	63.1	0.58	0.46	0.91	0.56
Slaughter	108.0	110.0	106.0	112.0	1.14	0.42	< 0.001	0.56
<i>ADFI, kg/d</i>								
Grower period	1.7	1.8	1.7	1.8	0.05	0.30	0.03	0.66
Finisher period	2.7	2.8	2.6	2.9	0.08	0.73	< 0.001	0.80
<i>Total feed intake, kg</i>								
Grower period	86.6	82.8	83.2	86.2	1.42	0.07	0.06	0.41
Finisher period	135.0	131.8	125.7	141.1	4.32	0.59	< 0.01	0.20
<i>Gain-to-feed ratio</i>								
Grower period	0.47	0.49	0.48	0.48	0.005	0.01	0.61	0.49
Finisher period	0.34	0.35	0.34	0.35	0.005	0.02	0.83	0.07
<i>Age, d</i>								
Grower period	76	72	75	74	2.1	0.10	0.59	0.48
Finisher period	129	119	122	117	2.7	< 0.0001	0.12	0.78
Slaughter	177	159	171	165	3.6	< 0.001	0.21	0.36

Effect of classifying the pigs based on the brain-to-liver weight ratio (BrW/LW) at birth and sex on growth performance traits

¹ Category: IUGR = pigs with the highest BrW/LW; NORM: pigs with the lowest BrW/LW

² P-value for the main effect of the category, sex, and their interaction

³ Pooled SEM

⁴ ADFI average daily feed intake, expressed as g per day

Faecal microbiota

A total of 3,436,549 sequence reads were attributed to a total of 9,256 Amplicon Sequence Variants (ASV) distributed among all samples, see Supplementary Table 2, Additional File 1. The relative rarefaction curves illustrated the tendency to plateau for all the samples,

suggesting that the sequencing depth was sufficient to describe the variability within the microbial communities analysed among the samples (see Supplementary Fig. 1, Additional File 1). One sample from the NORM group was removed from the analysis due to the low number of reads. The taxonomic assignment resulted in the

Table 3 Body composition at weaning, end of the starter period and end of the finisher period

Item ⁴	Category ¹		Sex		SEM ³	P-value ²		
	IUGR	NORM	Females	Castrates		Category	Sex	Category × Sex
<i>Bone mass, %</i>								
Weaning	2.35	2.21	2.28	2.28	0.114	0.50	0.97	0.15
End of starter period	1.65	1.80	1.74	1.71	0.017	<0.001	0.07	0.68
End of finisher period	2.04	2.05	2.15	1.94	0.065	0.96	<0.001	0.56
<i>Bone mineral density, %</i>								
Weaning	0.008	0.005	0.006	0.006	0.0007	0.03	0.87	0.29
End of starter period	0.002	0.003	0.002	0.002	0.00005	0.02	0.17	0.90
End of finisher period	0.0012	0.0011	0.0012	0.0011	0.00002	0.14	<0.01	0.06
<i>Lean mass, %</i>								
Weaning	86.7	87.7	87.0	87.4	0.58	0.27	0.65	0.90
End of starter period	90.0	90.1	90.2	90.0	0.19	0.53	0.37	0.97
End of finisher period	78.8	79.7	80.7	77.8	0.50	0.59	0.07	0.02
<i>Fat mass, %</i>								
Weaning	11.0	10.1	10.4	10.7	0.61	0.41	0.64	0.91
End of starter period	8.4	8.1	8.1	8.4	0.20	0.22	0.31	0.95
End of finisher period	19.1	18.3	17.2	20.2	0.52	0.47	0.04	0.01

Effect of classifying the pigs based on the brain-to-liver weight ratio (BrW/LW) at birth and sex on the relative bone mass, bone mineral density, lean mass and fat mass at weaning, end of the starter period, and end of the finisher period

¹ Category: IUGR = pigs with the highest BrW/LW; NORM: pigs with the lowest BrW/LW

² P-value for the main effect of the category, sex, and their interaction

³ Pooled SEM

⁴ Percentage of total mass

Number of pigs scanned at weaning: IUGR = 12; NORM = 11; females = 15; castrates = 8; IUGR females = 8; IUGR castrates = 4; NORM females = 7; NORM castrates = 4

Number of pigs scanned in the starter period: IUGR = 12; NORM = 12; females = 12; castrates = 12; IUGR females = 7; IUGR castrates = 5; NORM females = 5; NORM castrates = 7

Number of pigs scanned in the finisher period: IUGR = 11; NORM = 11; females = 11; castrates = 11; IUGR females = 6; IUGR castrates = 5; NORM females = 5; NORM castrates = 6

Significant interaction between category and sex: IUGR females: 79.5^{abc}%; NORM females: 81.8^b%; IUGR castrates: 78.1^{ac}%; NORM castrates: 77.6^c%. Different letters (a, b, c) indicate statistically significant ($P < 0.05$) differences between the groups

Significant interaction between category and sex: IUGR females: 18.3^{ab}%; NORM females: 16.0^b%; IUGR castrates: 19.9^a%; NORM castrates: 20.5^a%. Different letters (a, b) indicate statistically significant ($P < 0.05$) differences between the groups

identification of 22 phyla, 117 families, and 338 genera. The most abundant phyla were *Firmicutes* (70.89 ± 14%) and *Bacteroidota* (21.11 ± 11%). The most abundant families were *Lactobacillaceae* (20.93 ± 17%), *Lachnospiraceae* (12.34 ± 6%), and *Prevotellaceae* (11.67 ± 9%). The most represented genera were *Lactobacillus* (16.63 ± 15%), *Streptococcus* (4.76 ± 6%), and HT002 (3.69 ± 6%).

Line plots showing the Alpha diversity values within the IUGR and NORM groups across different time points are displayed in Fig. 1. The time (i.e., age of the pigs) significantly affected the Chao1 and Shannon indices ($P < 0.001$ and $P < 0.001$, respectively), while the InvSimpson index was not affected. No effects were observed for the category or for the interaction between category and time. Separate models within each time point were then fitted. No significant differences between the IUGR and NORM categories were observed at T1, T2, and T3, except for a tendency

for higher Chao1 ($P = 0.066$) and Shannon indices ($P = 0.053$) in the IUGR group compared to the NORM group at T2.

The Adonis test carried out on Beta diversity showed a significant effect of the category ($P = 0.011$, $R^2 = 0.017$), time ($P = 0.001$, $R^2 = 0.185$), their interaction ($P = 0.016$, $R^2 = 0.039$), and by the litter of origin ($P = 0.016$, $R^2 = 0.039$). Samples tended to cluster according to the IUGR/NORM status within each time point, as evidenced by the NMDS plot in Fig. 2. Separate Adonis models on the Beta diversity matrix at each time point were then carried out. At T1, the Beta diversity was affected by the category ($P = 0.002$, $R^2 = 0.083$) and litter of origin ($P = 0.001$, $R^2 = 0.616$). At T2, a tendency was recorded ($P = 0.079$, $R^2 = 0.068$) for the category, and no differences were observed for the litter of origin. At T3, the Beta diversity was affected by the category ($P = 0.027$, $R^2 = 0.066$), and a trend was observed for the

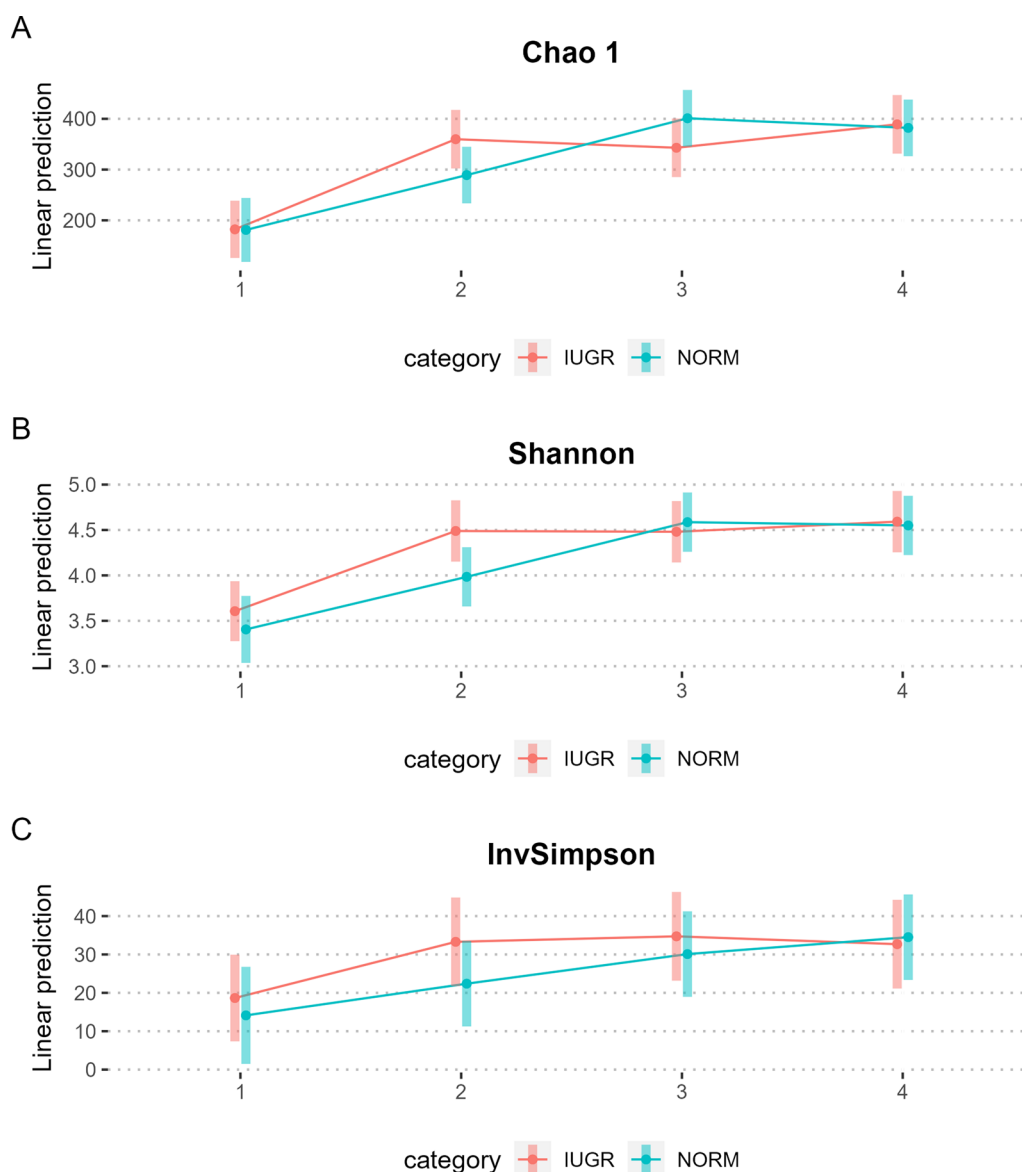


Fig. 1 Microbial Alpha diversity within IUGR and NORM categories over time. Line plots showing the Alpha diversity values within each category (IUGR=pigs affected by intrauterine growth restriction; NORM=normal pigs) over time, measured with the Chao1 (panel A), Shannon (panel B), and InvSimpson (panel C) indexes. T1=day 16±0.6; T2=day 63±8.6; T3=day 119±11.4; T4=day 162±14.3 of age. The time significantly affected the Chao1 ($P<0.001$) and Shannon ($P<0.001$) indices

litter of origin ($P=0.082$, $R^2=0.301$). At T4, no effect was observed on Beta diversity.

To identify which taxa contributed to the differences among the categories, the LEfSe algorithm on the data aggregated at the genus levels was applied within each time point. No differences were observed at T4. The microbiological markers observed at T1, T2, and T3 are shown in Fig. 3A–C, respectively. At T1, the IUGR group showed higher abundances of *Clostridium sensu stricto 1* (LDA score=4.55; $P_{\text{adj}}=0.029$) and *Romboutsia*

(LDA score=4.04; $P_{\text{adj}}=0.047$), while the NORM group was characterised by a higher abundance of *Ruminococcus* (LDA score=4.39; $P_{\text{adj}}=0.010$). At T2, IUGR pigs had higher abundances of *Prevotellaceae NK3B31 group* (LDA score=4.5; $P_{\text{adj}}=0.021$), *Rikenellaceae RC9 gut group* (LDA score=4.49; $P_{\text{adj}}=0.030$), and *Alloprevotella* (LDA score=4.26; $P_{\text{adj}}=0.030$), while the NORM group showed a higher abundance of HT002 (LDA score=4.27; $P_{\text{adj}}=0.048$), an uncultured genus of *Lactobacillaceae* family. At T3, the IUGR group was characterised by

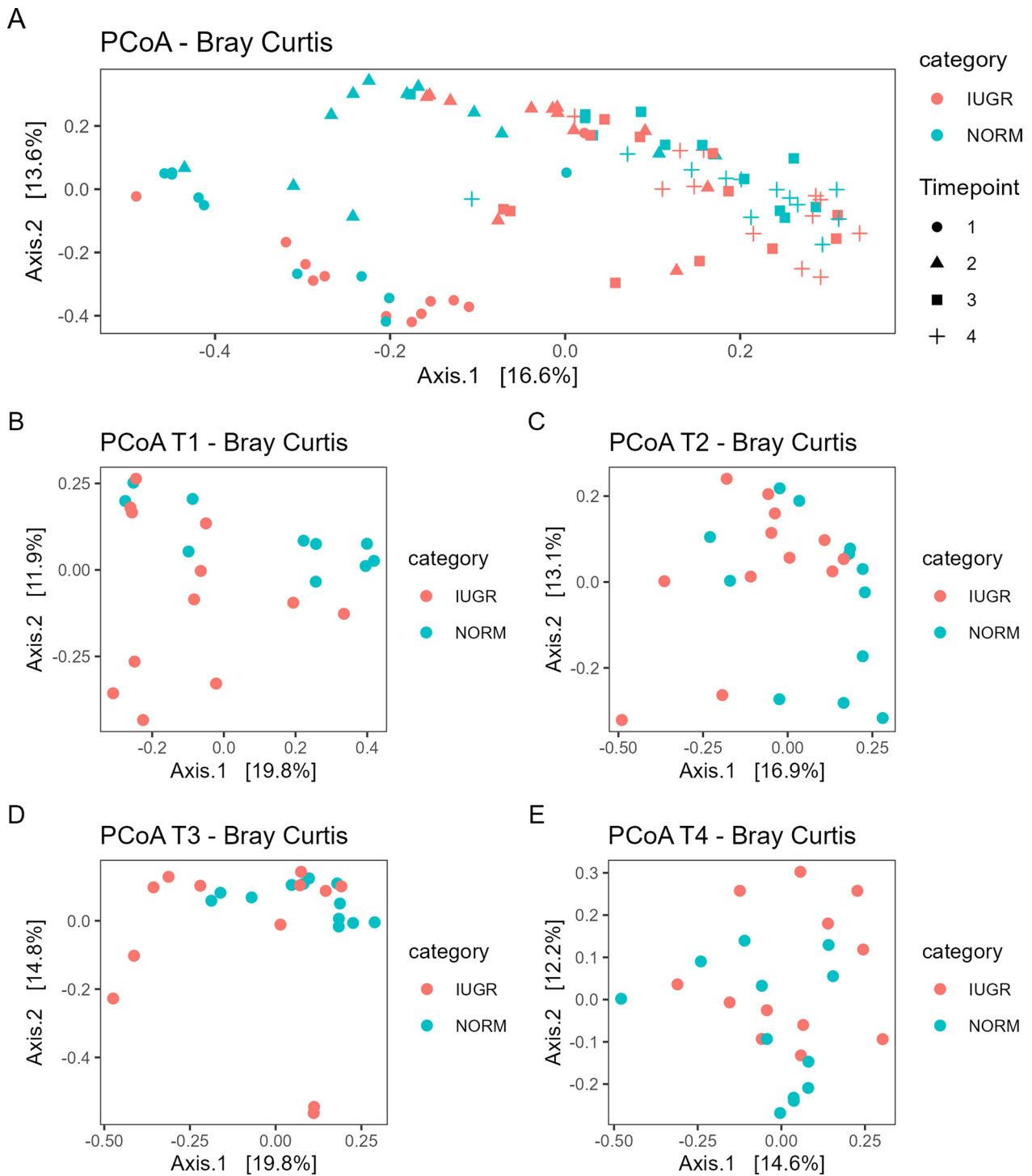


Fig. 2 Microbial Beta diversity within IUGR and NORM categories over time. NMDS plot using Bray–Curtis dissimilarity matrix showing the differences in bacterial composition between pigs affected by intrauterine growth restriction (IUGR) and normal pigs (NORM) over time (panel A) and at T1 (panel B), T2 (panel C), T3 (panel D), and T4 (panel E). T1 = day 16 ± 0.6; T2 = day 63 ± 8.6; T3 = day 119 ± 11.4; T4 = day 162 ± 14.3 of age

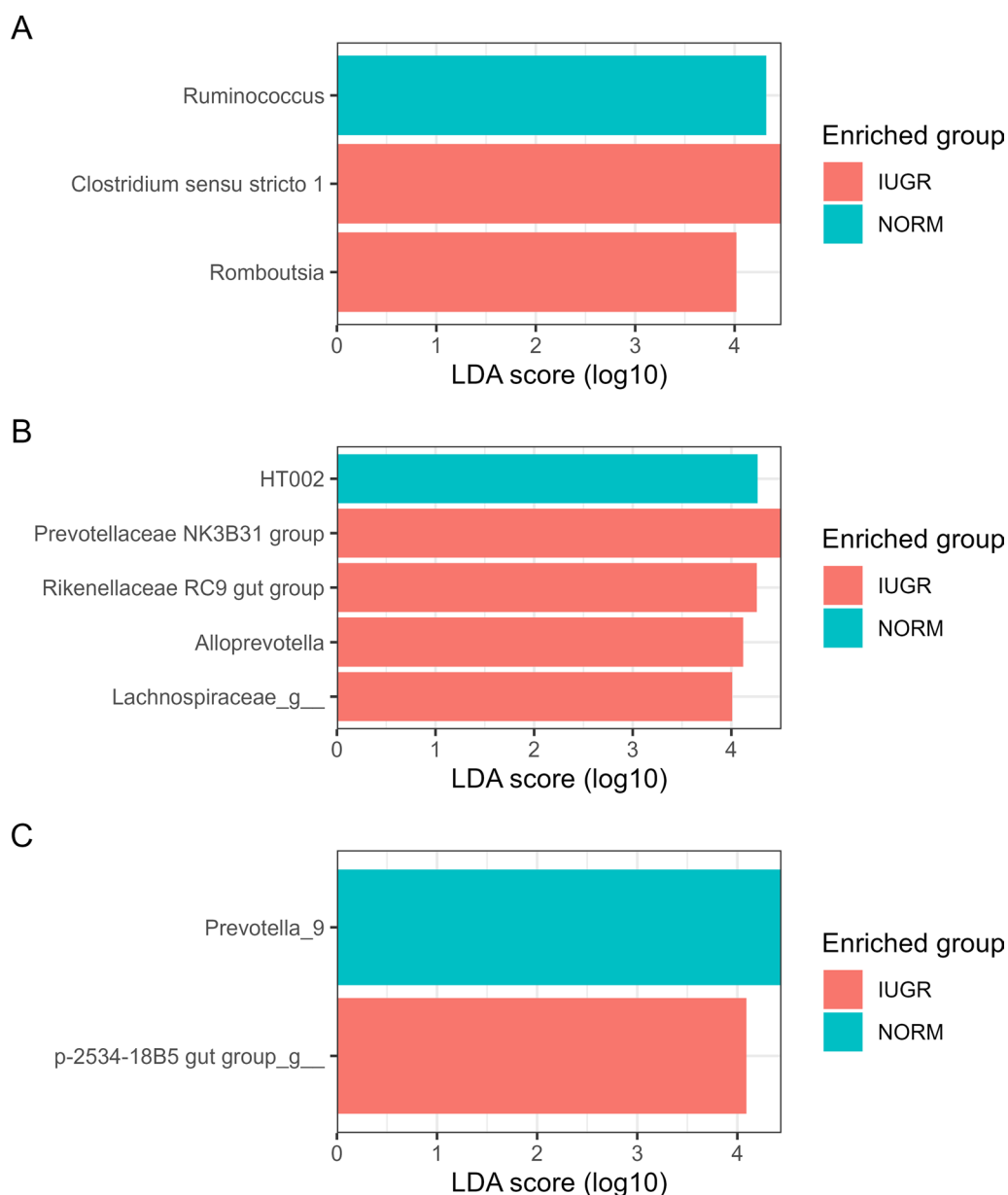


Fig. 3 Microbiological markers observed over time in IUGR and NORM pigs. The LDA plot shows the bacterial markers characterising pigs affected by intrauterine growth restriction (IUGR) and normal pigs (NORM) at T1 (panel A), T2 (panel B), and T3 (panel C). No differences were observed at T4. T1 = day 16 ± 0.6 ; T2 = day 63 ± 8.6 ; T3 = day 119 ± 11.4 ; T4 = day 162 ± 14.3 of age

a higher abundance of p-2534-18B5 gut group (LDA score = 4.3, $P_{adj} = 0.03$) from the *Bacteroidales* order, while the NORM group was characterised by a higher abundance of *Prevotella_9* (LDA score = 4.6; $P_{adj} < 0.001$).

Plasma metabolome

From the plasma samples of 24 pigs (IUGR = 12, NORM = 12) collected at T1, 65 metabolites were analysed. Of the 65 metabolites measured at T1, 44 were in the quantitation range for each sample and were analysed

statistically. The others were not detectable in any or most of the plasma samples after centrifugation and were excluded from the statistical analysis (Supplementary Table 3, Additional File 1). Only leucine and 2-aminobutyrate exhibited significant differences between IUGR and NORM pigs at T1, with IUGR pigs showing lower plasma concentrations of both metabolites compared to the NORM group ($P < 0.01$). Nevertheless, after applying the Benjamini–Hochberg correction, none of the metabolites demonstrated significant differences between the

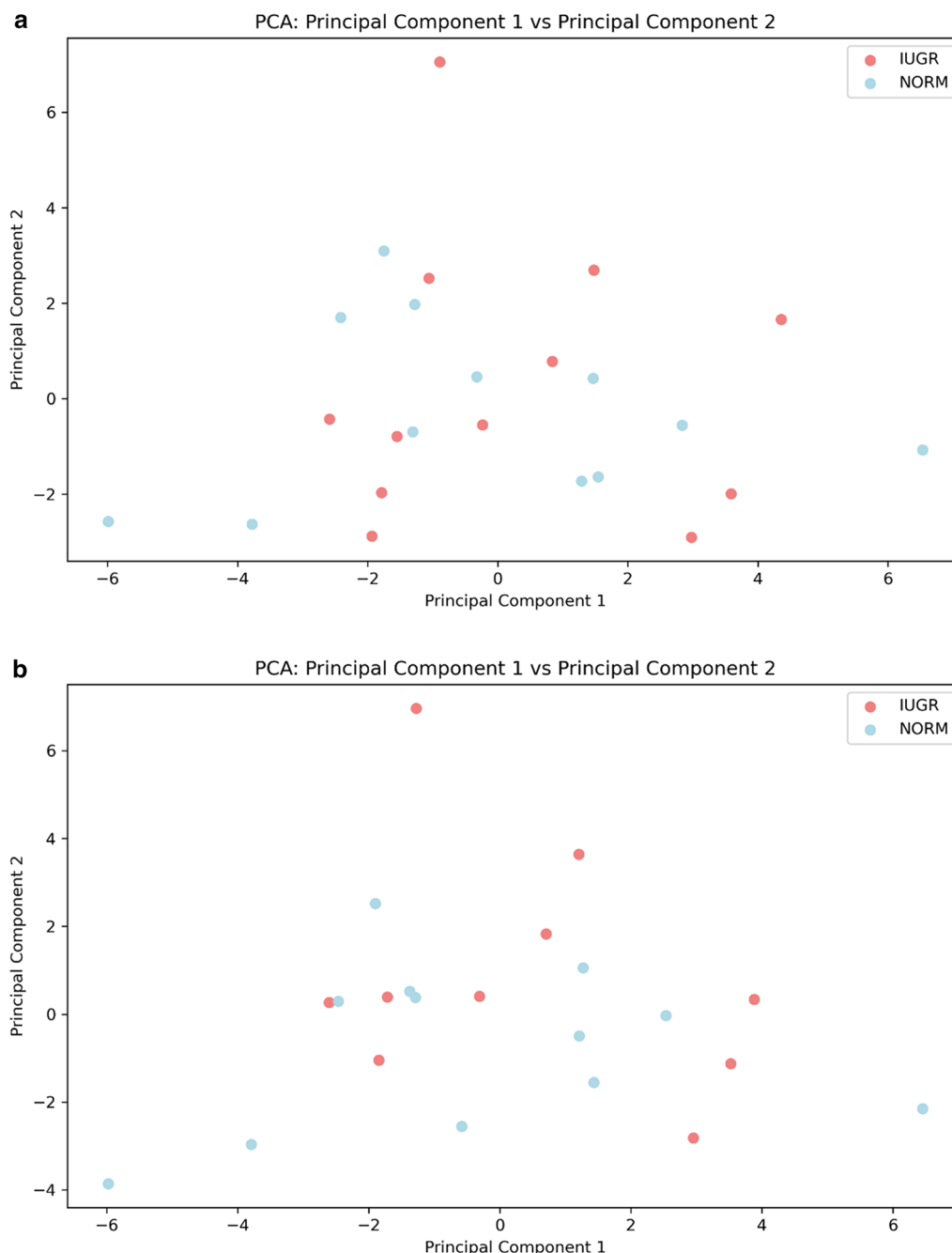


Fig. 4 Principal component analysis of the metabolomic data at T1. Scatter plot visualising the principal components of the unsupervised principal component analysis (PCA) of the metabolomic data from the samples collected on day 16 ± 0.6 (T1) of age before **(a)** and after **(b)** the removal of outliers. Each data point is represented by its coordinates in the first and second principal components. The data points belonging to the normal pigs (NORM) are plotted in blue, and those belonging to pigs affected by intrauterine growth restriction (IUGR) are plotted in red. Samples do not group together according to the IUGR/NORM status in the scatter plot of the PCA first principal plan

IUGR and NORM pigs. The PCA analysis identified two outliers (both from the IUGR group), and no spontaneous sample grouping was observed (Fig. 4, Panel A). Even after the removal of outliers, no significant variations were observed in the metabolite concentrations between

the IUGR and NORM pigs, and the PCA analysis continued to show a lack of spontaneous grouping of the samples (Fig. 4, Panel B).

The OPLS-DA model enabled good group discrimination ($R^2Y=0.85$, Fig. 5, Panel A) but weak predictive

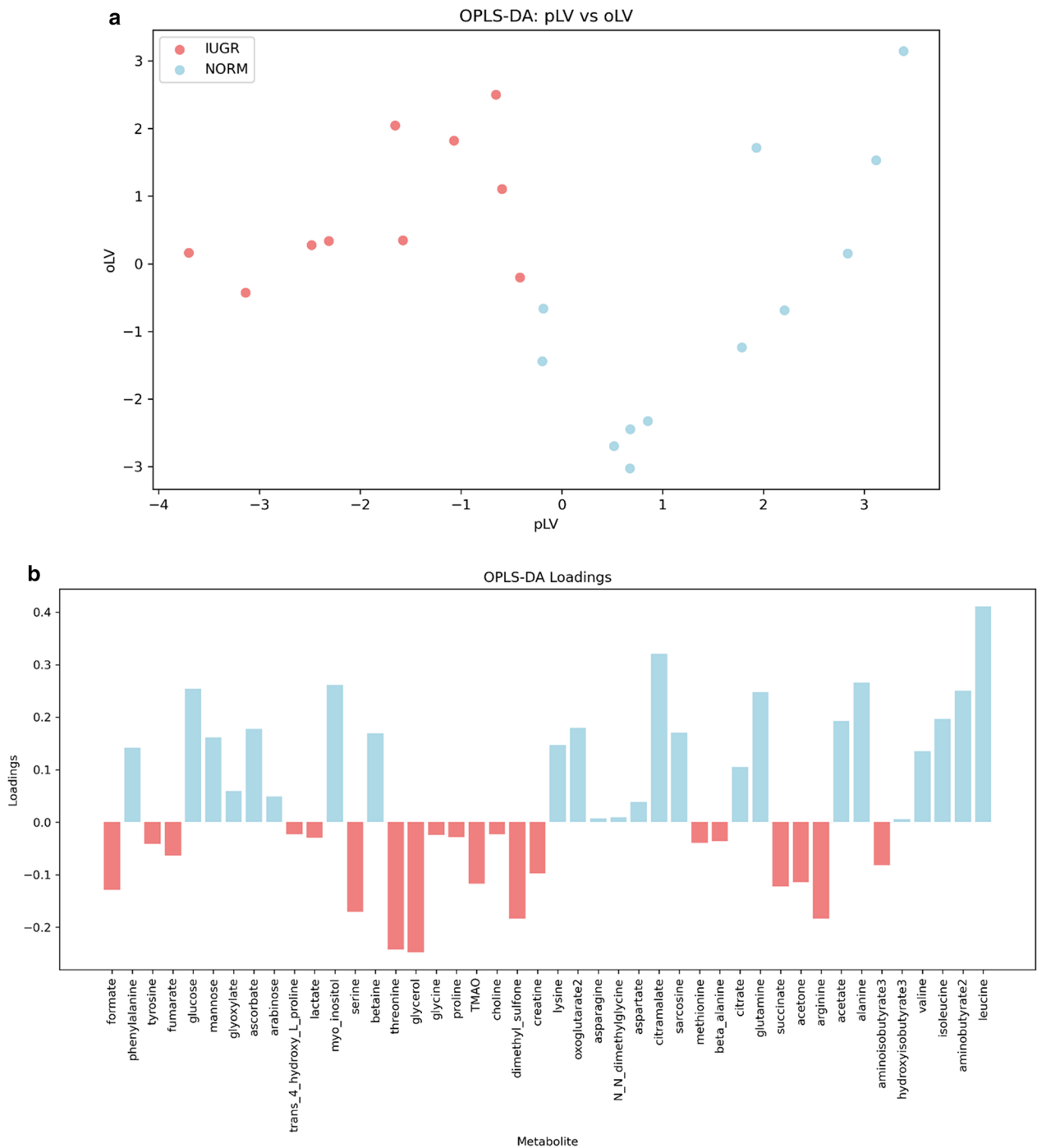


Fig. 5 Orthogonal partial least squares discriminant analysis of the metabolomic data at T1. **a** Scatter plot visualising the principal components of the supervised orthogonal partial least squares discriminant analysis (OPLS-DA) of the metabolomic data from the plasma samples collected on day 16 ± 0.6 (T1) of age after the removal of outliers. Each data point is represented by its coordinates in two components: predictive latent variable (pLV) and orthogonal latent variable (oLV). The data points belonging to the normal pigs (NORM) are plotted in blue, and those belonging to pigs affected by intrauterine growth restriction (IUGR) are plotted in red. The samples group together according to the IUGR/NORM status in the scatter plot of the OPLS-DA first principal plan. **b** OPLS-DA loadings plot of the metabolomic data from the plasma samples collected at T1 after the removal of outliers; x-axis: metabolites present in the plasma; y-axis: loadings for each metabolite. Loadings indicate the contribution of each metabolite to the separation between the two groups: pigs affected by intrauterine growth restriction (IUGR) and normal pigs (NORM). Positive loadings indicate that higher levels of the metabolite are associated with the NORM groups, while negative loadings indicate higher levels in the IUGR group. The metabolites with the highest positive and negative loadings contribute the most to the separation between the two groups

ability and a high risk of overfitting ($Q^2Y = -0.47$, Q^2Y perm test = 0.04). Plasma metabolites that contributed the most to the separation between the IUGR and NORM groups are shown in the OPLS-DA loading plot in Fig. 5, Panel B. None of the metabolites could significantly differentiate the two groups as all had a VIP score of less than 1 in the OPLS-DA analysis (Table 4).

From the plasma samples of 24 pigs (IUGR = 12, NORM = 12) collected at T2, 65 metabolites were analysed. Of the 65 metabolites measured at T2, 44 were in the quantitation range and were analysed statistically. The others were not detectable in any or most of the plasma samples and were excluded from the statistical analysis (see Supplementary Table 4, Additional File 1). Arabinose, arginine, ascorbate, asparagine, creatine, dimethyl-sulfone, glyoxylate, proline, and sarcosine exhibited significant differences between IUGR and NORM pigs at T2. Nevertheless, after applying the Benjamini–Hochberg correction, only asparagine was significantly different between the IUGR and NORM groups. The PCA analysis showed one outlier (from the NORM group) and a tendency of the samples to spontaneously group (Fig. 6, Panel A). After the removal of the outlier, asparagine was still the only metabolite showing significant variations between IUGR and NORM pigs. Compared with the NORM group, IUGR pigs had significantly lower ($P < 0.05$ and t -statistic $\neq 0$) concentrations of asparagine at T2 (Fig. 7). The PCA analysis continued to show a tendency for spontaneous sample grouping after the removal of the outlier (Fig. 6, Panel B). The OPLS-DA model enabled good group discrimination ($R^2Y = 0.77$, Fig. 8, Panel A) but weak predictive ability and a high risk of overfitting ($Q^2Y = -1.48$, Q^2Y perm test = 0.05). Plasma metabolites that contribute the most to the separation between the IUGR and NORM groups are shown in the OPLS-DA loading plot in Fig. 8, Panel B. None of the plasma metabolites showed a $VIP > 1.0$ in the OPLS-DA analysis (Table 5).

Relationship between faecal microbiota and plasma metabolome

In the global analysis, which included all metabolites and bacterial genera, no significant correlations ($r > 0.6$ and $P < 0.05$) between metabolites and bacteria were identified at either time point (T1, T2) after correcting for multiple comparisons. The same result was found when analysing all metabolites and only the bacterial genera that differed between IUGR and NORM pigs. Finally, even in a targeted analysis focusing exclusively on metabolites and bacterial genera that differed between IUGR and NORM pigs, no significant correlations were observed at any time point following correction for multiple comparisons.

Table 4 Metabolites of interest at day 16 ± 0.6 (T1)

Metabolite	VIP	Loading
Tyrosine	0.20	-0.04
Leucine	0.20	0.04
Aspartate	0.19	0.04
Sarcosine	0.19	0.17
Alanine	0.18	0.27
Myo-inositol	0.16	0.26
Serine	0.16	0.17
Citramalate	0.15	0.32
2-Oxoglutarate	0.15	0.18
Glycerol	0.15	0.25
Acetate	0.14	0.19
2-Aminobutyrate	0.14	0.25
Threonine	0.13	-0.24
Beta-alanine	0.13	-0.04
Arginine	0.13	-0.18
Phenylalanine	0.13	0.14
Lysine	0.13	0.14
Glucose	0.12	0.25
Glyoxylate	0.12	0.06
Glutamine	0.12	0.25
Isoleucine	0.11	0.19
3-Hydroxyisobutyrate	0.11	0.01
TMAO	0.11	-0.12
Citrate	0.10	0.10
Dimethyl-sulfone	0.09	0.18
Glycine	0.09	-0.02
Ascorbate	0.09	0.18
Mannose	0.08	0.16
Betaine	0.08	0.17
Asparagine	0.08	0.01
Succinate	0.08	-0.12
Formate	0.07	-0.13
Creatine	0.07	-0.09
Valine	0.07	0.14
3-Aminoisobutyrate	0.06	-0.08
Acetone	0.06	-0.11
Methionine	0.06	-0.04
N,N-dimethylglycine	0.05	0.01
Arabinose	0.04	0.05
Fumarate	0.03	-0.06
Trans-4-hydroxy-L-proline	0.02	0.02
Proline	0.02	-0.03
Lactate	0.02	-0.03
Choline	0.01	-0.02

Identification of metabolites of interest at day 16 ± 0.6 (T1) of age through the combination of the variable importance in the projection (VIP) and the loading between the metabolite in the X matrix and the predictive latent variable (pLV) of the OPLS-DA model. Metabolites are sorted by decreasing VIP

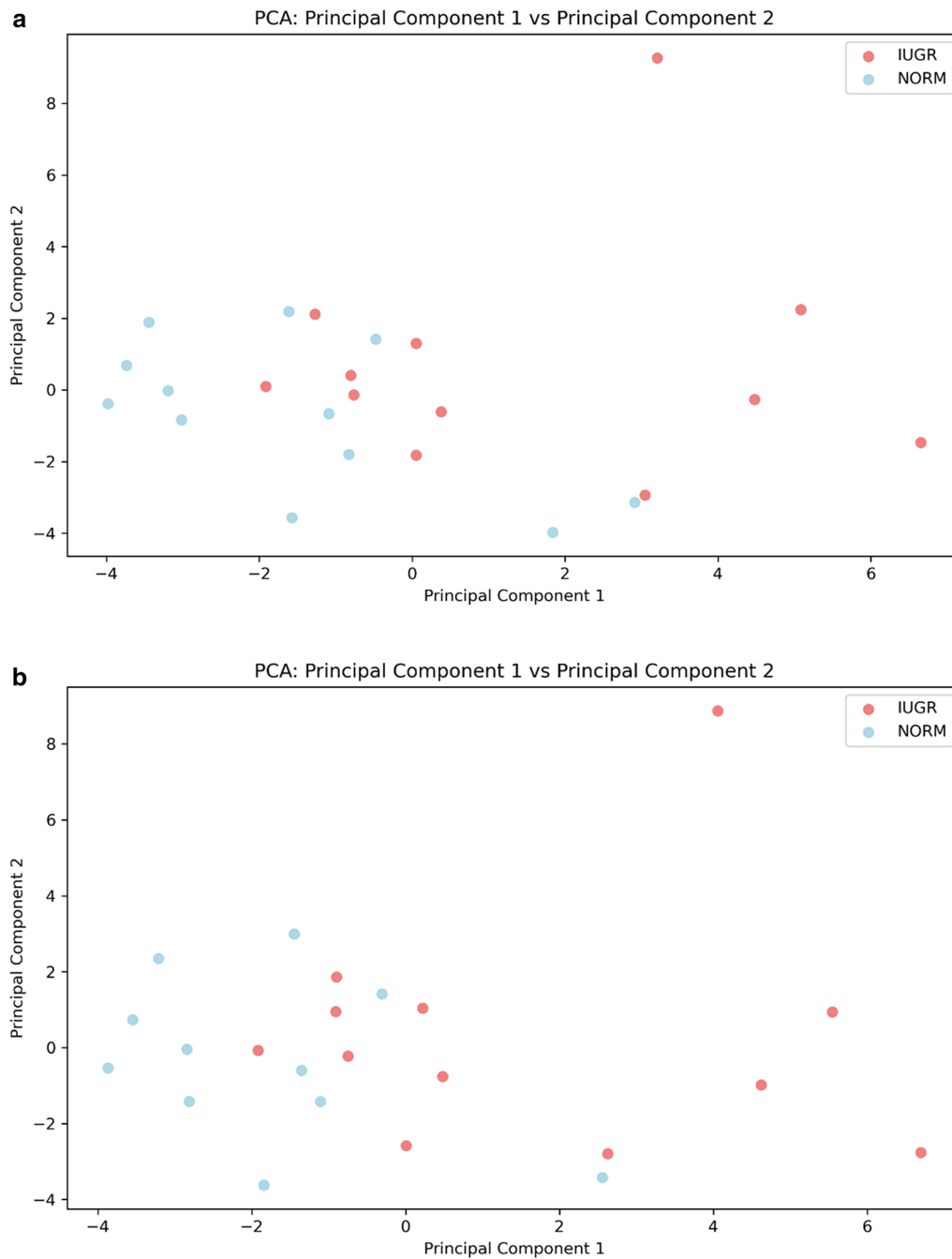


Fig. 6 Principal component analysis of the metabolomic data at T2. Scatter plot visualising the principal components of the unsupervised principal component analysis (PCA) of the metabolomic data from the samples collected on day 63 ± 8.6 (T2) of age before **(a)** and after **(b)** the removal of outliers. Each data point is represented by its coordinates in the first and second principal components. The data points belonging to the normal pigs (NORM) are plotted in blue, and those belonging to pigs affected by intrauterine growth restriction (IUGR) are plotted in red. Samples tend to group together according to the IUGR/NORM status in the scatter plot of the PCA first principal plan

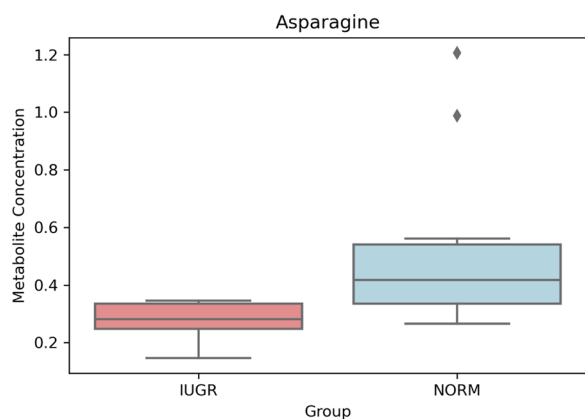


Fig. 7 Plasma asparagine concentration of IUGR and NORM pigs at T2. Box plot showing the different plasma asparagine concentrations observed between pigs affected by intrauterine growth restriction (IUGR) and normal pigs (NORM) at day 63 ± 8.6 (T2) of age; x-axis: IUGR: 12 piglets with the highest brain-to-liver weight ratio (BrW/LW); NORM: 12 piglets with lower BrW/LW; y-axis: plasma metabolite concentration (mmol/L)

Discussion

Microbiota and metabolome analyses hold the potential to identify biomarkers of IUGR and offer insights into the underlying mechanisms of this condition. To our knowledge, this is the first time the effect of IUGR on physiological traits has been evaluated based on the piglets' BrW/LW at birth.

Effect of intrauterine growth restriction on average daily gain

The variations in performance observed in this study align with the well-known differences between IUGR and normal pigs reported in the literature and demonstrated in our previous study in a larger population [21]. IUGR pigs displayed a decreased ADG from birth to the end of the grower period. Nevertheless, during the finisher period, the ADG remained comparable between IUGR pigs and their NORM counterparts. Various studies have demonstrated a reduction in ADG among IUGR pigs, from birth to weaning [36], from birth to the growing phase [37, 38], and from birth to slaughter [2, 39]. Similar to our findings, Alvarenga et al. [38] reported that IUGR pigs, identified by low birth weight, initially exhibited lower ADG from birth to the grower phase. However, by day 150, their ADG became comparable to that of normal pigs. These findings confirm the diminishing influence of birth weight on ADG over time [40, 41].

Effect of intrauterine growth restriction on body composition determined by dual X-ray absorptiometry

In the current experiment, there was no difference between IUGR and NORM pigs in the bone, lean, and fat tissue when expressed as a percentage of the body mass at weaning. These results align with our previous study [21] conducted on a larger population and are consistent with the study of Lynegaard [37], in which no differences in fat or muscle percentage were found in relation to BW at 24 days of age between IUGR and normal pigs. However, the bone mineral density was significantly higher in IUGR pigs compared to their NORM counterparts at weaning. The comparable percentage of bone in IUGR and NORM pigs and the higher bone mineral density in the IUGR group may suggest a certain level of compensatory mechanisms or adaptive responses to the growth restriction experienced in the uterus.

At the end of the starter period, while the percentages of lean and fat mass in the body remained similar between IUGR and NORM pigs, there were significant differences in the proportions of bone and bone mineral density. Specifically, IUGR pigs exhibited lower proportions of bone and bone mineral density in relation to body mass compared to their NORM counterparts. These findings are consistent with research conducted on humans and rats, which demonstrated reduced bone mass and density and increased risk for osteoporosis in IUGR-affected subjects [42]. Pigs with compromised skeletal development may be more susceptible to bone injuries, such as fractures, leading to a reduction in animal welfare and an increase in veterinary costs. The observed fluctuations in bone mineral density during various developmental stages in IUGR compared to NORM pigs indicate a dynamic and possibly adaptive reaction to the modification imposed by growth restriction during foetal development. However, further research is necessary to understand the underlying mechanisms causing these variations and the potential impact on skeletal health.

At the end of the finisher period, IUGR castrated pigs displayed a lower proportion of lean tissue and a higher percentage of fat compared to NORM females. Regarding lean and fat deposition, several studies reported that pigs with a low birth weight had a decreased percentage of muscle and an increased percentage of body fat than their heavier littermates at slaughter [6, 20, 43]. However, in this study, there were no significant differences between IUGR and NORM pigs of the same sex. Generally, female pigs have a higher proportion of lean tissue and lower fat content compared to castrated pigs. This variation in body composition between females and castrates is well-established in the literature [44, 45]. In our

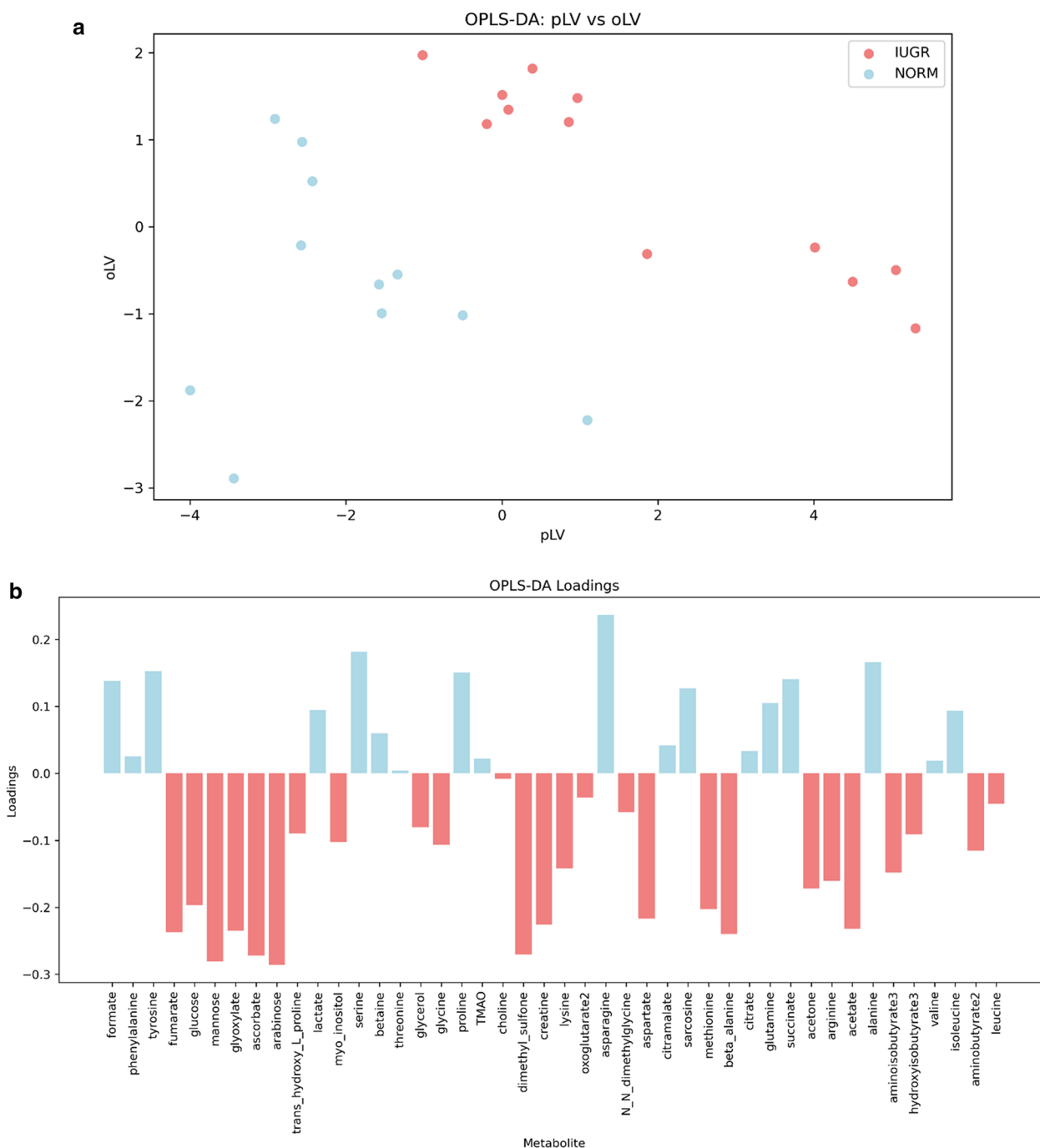


Fig. 8 Orthogonal partial least squares discriminant analysis of the metabolomic data at T2. **a** Scatter plot visualising the principal components of the supervised orthogonal partial least squares discriminant analysis (OPLS-DA) of the metabolomic data from the plasma samples collected on day 63 ± 8.6 (T2) of age after the removal of outliers. Each data point is represented by its coordinates in two components: predictive latent variable (pLV) and orthogonal latent variable (oLV). The data points belonging to the normal pigs (NORM) are plotted in blue, and those belonging to pigs affected by intrauterine growth restriction (IUGR) are plotted in red. The samples group together according to the IUGR/NORM status in the scatter plot of the OPLS-DA first principal plan. **b** OPLS-DA loadings plot of the metabolomic data from the plasma samples collected at after removal of the outlier; x-axis: metabolites present in the plasma; y-axis: loadings for each metabolite. Loadings indicate the contribution of each metabolite to the separation between the two groups: pigs affected by intrauterine growth restriction (IUGR) and normal pigs (NORM). Positive loadings indicate that higher levels of the metabolite are associated with the NORM groups, while negative loadings indicate higher levels in the IUGR group. The metabolites with the highest positive and negative loadings contribute the most to the separation between the two groups

Table 5 Metabolites of interest at day 63 ± 8.6 (T2)

Metabolite	VIP	Loading
Asparagine	0.19	-0.24
Mannose	0.19	0.28
3-Aminoisobutyrate	0.18	0.15
Beta-alanine	0.18	0.24
Sarcosine	0.17	-0.13
Proline	0.16	-0.15
Fumarate	0.15	0.24
Arabinose	0.15	0.29
Ascorbate	0.14	0.27
2-Aminobutyrate	0.14	0.12
Aspartate	0.13	0.22
Succinate	0.13	-0.14
Glycine	0.13	0.11
Myo-inositol	0.13	0.10
Dimethyl-sulfone	0.12	0.27
Isoleucine	0.12	-0.09
Acetate	0.12	0.23
Creatine	0.11	0.23
Acetone	0.11	0.17
Methionine	0.11	0.20
Glyoxylate	0.11	0.23
Citrate	0.11	-0.03
Arginine	0.10	0.16
Tyrosine	0.09	-0.15
Glucose	0.09	0.20
TMAO	0.09	-0.02
Serine	0.08	-0.18
Phenylalanine	0.08	-0.03
Alanine	0.08	-0.17
Trans-4-hydroxy-L-proline	0.08	0.09
Lactate	0.07	-0.09
Formate	0.07	-0.14
Glycerol	0.07	0.08
Lysine	0.07	0.14
2-Oxoglutarate	0.06	0.04
Citramalate	0.06	-0.04
Glutamine	0.06	-0.10
Threonine	0.06	-0.00
N,N-dimethylglycine	0.05	0.06
3-Hydroxyisobutyrate	0.04	0.09
Leucine	0.04	0.05
Choline	0.04	0.01
Betaine	0.03	-0.06
Valine	0.01	-0.02

Identification of metabolites of interest at day 63 ± 8.6 (T2) of age through the combination of the variable importance in the projection (VIP) and the loading between the metabolite in the X matrix and the predictive latent variable (pLV) of the OPLS-DA model. Metabolites are sorted by decreasing VIP

study, this difference was even stronger when comparing castrated pigs exposed to IUGR to NORM females.

Effect of intrauterine growth restriction on faecal microbiota

In this study, faecal samples were collected from IUGR and NORM pigs at different time points and analysed for microbiota composition. The objective was to provide insights into the dynamic profile of faecal microbiota in pigs affected by IUGR compared to normal pigs across different developmental stages. At the phylum level, the faecal microbiota of both IUGR and NORM pigs was dominated by *Firmicutes* and *Bacteroidetes* at all time points, which is consistent with the previous literature [46–48]. Unlike other studies, the Alpha diversity of the faecal microbiota in the lactation, starter, grower, and finisher periods was not affected by IUGR status in our experiment, except for a tendency for a higher Alpha diversity in the IUGR group at the end of the starter period. Zhang et al. [10] reported the Alpha diversity of the jejunal microbiota in IUGR piglets, defined by their birth body weight, to be significantly lower than that of control piglets at 7 and 21 days of age, suggesting a dysbiosis in the gut of IUGR piglets during the lactation period. By contrast, Xiong et al. [39] observed that the Alpha diversity of the jejunum and ileum microbiota in IUGR pigs, identified based on their birth weight, was significantly higher than in normal pigs at 25, 50, and 100 kg BW, indicating a more diversified intestinal microbiota in the IUGR pigs during the grower-finisher phase.

In our study, the Beta diversity of the faecal microbiota across the lactation, starter, and grower periods was significantly affected by IUGR status, with the samples clustering according to the category within each time point. Accordingly, in Xiong et al.'s [39] study, Beta diversity analysis showed that IUGR pigs had a different microbial community in the small intestine at 25, 50, and 100 kg BW compared to normal pigs. Regarding the differential abundance analysis at the genus level, our findings revealed higher abundances of the genera *Clostridium sensu stricto 1* and *Romboutsia* in the IUGR group during the lactation period, while the NORM group was characterised by a higher abundance of *Ruminococcus*.

Ruminococcus belongs to the *Lachnospiraceae* family. These bacteria ferment dietary fiber and produce short-chain fatty acids, which play a beneficial role in the maintenance of intestinal health by improving barrier function and reducing inflammation [39, 49, 50]. The lower abundances of these bacteria in the IUGR pigs may contribute to the higher morbidity and mortality [51], as well as the reduced growth observed in IUGR compared to normal piglets in this and other studies [2, 21, 38].

At the end of the starter period, our results showed higher abundances of *Prevotellaceae* NK3B31 group, *Rikenellaceae* RC9 gut group, and *Alloprevotella* in the IUGR pigs, while the NORM group exhibited a higher abundance of HT002, an uncultured genus of the *Lactobacillaceae* family. Le Sciellour et al. [52] reported a positive link between the abundances of OTUs belonging to *Lactobacillaceae* and the digestibility of nitrogen and energy in grower–finisher pigs. In addition, *Lactobacillaceae* are also known to improve the health of the small intestine by modulating the gut microbiota, promoting beneficial fermentation, and exerting antagonistic activity against pathogens in pigs [53]. Considering the positive effect of *Lactobacillaceae* on the ability to digest feed, the lower abundances of bacteria belonging to this family may partly explain the reduced feed efficiency and ADG of IUGR compared to NORM pigs observed in this study and reported in the literature [2, 5, 21, 51]. However, at the same time point, the IUGR group showed higher abundances of bacteria belonging to the *Prevotellaceae* family. These bacteria can degrade complex carbohydrates and can help promote the intestinal health and growth of pigs [52, 54].

At the beginning of the finisher period, the IUGR group was characterised by a higher abundance of the *p*-2534-18B5 gut group from the *Bacteroidales* order, while the NORM group was characterised by a higher abundance of *Prevotella*_9. Bacteria belonging to the *Prevotellaceae* family, as mentioned above, are generally considered beneficial for gut health because they are involved in the fermentation of dietary fiber in the hindgut and the resultant production of short-chain fatty acids [54]. A reduction in these beneficial bacteria at the beginning of the finisher period may be associated with the poorer performance of IUGR-affected pigs compared to the NORM counterparts observed during the grower period.

The findings of our study suggest dynamic changes in faecal microbiota composition in pigs with IUGR compared to normal pigs across different developmental stages, independent of their diet. The observed differences in microbial composition, particularly in families associated with short-chain fatty acid production and gut health, may contribute to the impaired health and growth of IUGR pigs.

Effect of intrauterine growth restriction on plasma metabolome

In this study, plasma samples were collected from IUGR and NORM pigs during the lactation period and at the end of the starter phase to perform a metabolome analysis. Considering the restricted glucose availability and the increased adipocyte proliferation observed in IUGR foetuses [17–19], along with the ongoing enhanced

adipogenesis reported in postnatal life [19], we hypothesised differences in plasma metabolites associated with lipid and energy metabolism between IUGR and NORM piglets at both time points. As no significant differences in metabolites were observed between the IUGR and NORM pigs during the lactation period, we had to partially reject our hypothesis. Nevertheless, tyrosine and leucine emerged as the main contributors to the separation between the IUGR and NORM groups in the OPLS-DA analysis, showing lower concentrations in the plasma of IUGR piglets in the lactation period. This is in agreement with the findings of Lin et al. [55], who reported reduced leucine and tyrosine concentrations in the plasma of IUGR foetuses (defined by their foetal weight) in late gestation, and He et al. [11], who observed decreased serum tyrosine level in IUGR piglets, identified based on their birth body weight, at 21 days of age. Leucine, an essential branched-chain amino acid, acts as a nutrient signal to stimulate muscle protein synthesis in both newborns [56, 57] and weaned pigs [58]. Tyrosine, a non-essential aromatic amino acid, serves as a precursor for catecholamines (dopamine, norepinephrine, and epinephrine), crucial neurotransmitters in the central and peripheral nervous systems, and thyroid hormones, essential in the control of growth, development, and metabolism. The lower concentrations of leucine and tyrosine observed in IUGR-affected pigs may contribute to the reduced growth observed in this study, as well as the altered metabolism and impaired maturation of the nervous system reported in IUGR-affected piglets [2, 4, 59]. However, it is important to interpret the identified metabolites contributing to group separation with caution, as none of them showed a VIP > 1.0 in the OPLS-DA analysis in our study.

At the end of the starter period, only asparagine was significantly lower in the plasma of IUGR compared to NORM pigs, and it was the metabolite that contributed the most to the separation between the IUGR and NORM groups in the OPLS-DA analysis. Asparagine is a non-essential amino acid involved in energy and amino acid metabolism, as well as in protein synthesis [60]. Asparagine can act as a precursor for other amino acids of the arginine family, such as aspartate, glutamine, and glutamate, which are the major sources of ATP in mammalian enterocytes [61]. Additionally, asparagine contributes to immune function, as demonstrated by studies in weaned piglets, indicating its positive impact on the intestine and liver during inflammation [62, 63]. Considering the physiological functions of asparagine, a lower concentration of this amino acid could be associated with the reduced growth of IUGR pigs compared to their normal littermates and their higher susceptibility to diseases, as reported in several studies [2, 5, 51]. However,

other metabolites associated with lipid oxidation, energy, and protein metabolism, which showed changes between IUGR and normal pigs in other studies [11, 55], were not affected in the present study. The literature on metabolomic profiling in IUGR pigs across different growth stages is limited, and the interpretation of the results is challenging. There is currently no standardised definition of IUGR, and the diagnosis is often based solely on the BW of the foetus or the birth body weight of the piglet. This may be one reason for the contradictory findings [15].

Relationship between faecal microbiota and plasma metabolome

To investigate the interplay between faecal microbiota and plasma metabolome, correlation analyses between bacterial genera and metabolites were conducted in this study. However, despite using different approaches, our correlation analyses did not reveal any significant relationships between metabolites and bacterial genera. The absence of significant correlations may suggest a complex interaction between the faecal microbiota and plasma metabolome. It is also worth noting that many of the metabolites analyzed in this study are associated with the microbiota of the small intestine, while our analyses focused on correlations between plasma metabolites and faecal bacteria. This discrepancy could explain the absence of significant correlations. Understanding the link between gut or faecal microbiota and plasma metabolome profiles can provide insights into how microbial composition influences systemic metabolism in pigs.

Conclusion

In conclusion, our study confirmed that growth restriction in the uterus negatively affects the ADG from birth to the end of the grower period. Growth restriction during foetal development had a dynamic effect on bone mineral density across different developmental stages. In addition, IUGR had a significant and long-lasting impact on the faecal microbiota composition in pigs, from birth to the beginning of the finisher period. In contrast, growth restriction minimally affected the plasma metabolome profile of pigs at different growing stages. Identifying biomarkers associated with IUGR could provide novel insights into this condition, facilitating early interventions and effective management strategies. The successful treatment of the IUGR-affected pigs holds the potential to improve the overall efficiency of pig production systems.

Abbreviations

¹ H-NMR	Proton nuclear magnetic resonance
ADFI	Average daily feed intake
ADG	Average daily gain

BrW/LW	Brain-to-liver weight ratio
CT	Computed tomography
DXA	Dual-energy X-ray absorptiometry
GIT	Gastrointestinal tract
IUGR	Intrauterine growth restriction
LDA	Linear discriminant analysis
NMDS	Non-metric multidimensional scaling
OPLS-DA	Orthogonal projection to latent structures-discriminant analysis
PCA	Principal component analysis
pLV	Predictive latent variable
Q2Y	Predictive ability of the model
Q2Y-perm	Predictive ability of permuted models
R2Y	Goodness of fit of the model
VIP	Variable importance in the projection

Supplementary Information

The online version contains supplementary material available at <https://doi.org/10.1186/s42523-024-00358-9>.

Additional file 1

Acknowledgements

The authors thank the animal caretakers from the piggery for their technical support.

Author contributions

RR: acquisition, analysis, and interpretation of data; draft of the work GB: conception and design of the work, interpretation of data, and revision of the work, acquisition of the funding FC: analysis and interpretation of data and revision of the work PT: interpretation of data and revision of the work CO: conception and design of the work, acquisition and interpretation of data, and revision of the work.

Funding

This research received funding from the European Union's Horizon 2020 research and innovation programme under a Marie Skłodowska-Curie grant (agreement no. 955374).

Availability of data and materials

Additional files, raw sequence data, datasets and scripts used in the current study are available in Figshare (https://figshare.com/projects/Intrauterine_growth_restriction_defined_by_an_elevated_brain-to-liver_weight_ratio_affects_faecal_microbiota_composition_and_to_a_lesser_extent_plasma_metabolome_profile_at_different_ages_in_pigs/202746)

Declarations

Ethics approval

All the experimental procedures complied with Swiss animal welfare guidelines and were approved (experimental approval number 32751) by the Cantonal Veterinary Office of Fribourg (Switzerland).

Competing interests

The authors declare no competing interests.

Author details

¹Swine Research Unit, Agroscope, Route de La Tioleyre 4, 1725 Posieux, Switzerland. ²Department of Agricultural and Food Sciences (DISTAL), University of Bologna, Viale G Fanin 44, 40127 Bologna, Italy.

Received: 30 April 2024 Accepted: 16 November 2024

Published online: 19 February 2025

References

- Sharma D, Shastri S, Farahbakhsh N, Sharma P. Intrauterine growth restriction—part 1. *J Matern Fetal Neonatal Med.* 2016;29:3977–87.
- Santos TG, Fernandes SD, de Oliveira Araújo SB, Felicioni F, de Mérici Domingues e Paula T, Caldeira-Brant AL, Ferreira SV, de Paula Naves L, de Souza SP, Reis Furtado Campos PH, Chiarini-Garcia H, Neves Alvarenga Dias AL, Radicchi Campos Lobato de Almeida F. Intrauterine growth restriction and its impact on intestinal morphophysiology throughout postnatal development in pigs. *Sci Rep.* 2022;12:11810
- Oliviero C, Junnikkala S, Peltoniemi O. The challenge of large litters on the immune system of the sow and the piglets. *Reprod Domest Anim.* 2019;54:12–21.
- Shen L, Gan M, Zhang S, Ma J, Tang G, Jiang Y, Li M, Wang J, Li X, Che L. Transcriptome analyses reveal adult metabolic syndrome with intrauterine growth restriction in pig models. *Front Genet.* 2018;9:291.
- Wu G, Bazer F, Wallace J, Spencer T. Board-invited review: Intrauterine growth retardation: implications for the animal sciences. *J Anim Sci.* 2006;84:2316–37.
- Krueger R, Derno M, Goers S, Metzler-Zebeli BU, Nuernberg G, Martens K, Pfuhr R, Nebendahl C, Zeyner A, Hammon HM. Higher body fatness in intrauterine growth retarded juvenile pigs is associated with lower fat and higher carbohydrate oxidation during ad libitum and restricted feeding. *Eur J Nutr.* 2014;53:583–97.
- Moeser AJ, Pohl CS, Rajput M. Weaning stress and gastrointestinal barrier development: Implications for lifelong gut health in pigs. *Animal Nutrition.* 2017;3:313–21.
- Maynard CL, Elson CO, Hatton RD, Weaver CT. Reciprocal interactions of the intestinal microbiota and immune system. *Nature.* 2012;489:231–41.
- Wang H, Xu R, Zhang H, Su Y, Zhu W. Swine gut microbiota and its interaction with host nutrient metabolism. *Animal Nutr.* 2020;6:410–20.
- Zhang W, Ma C, Xie P, Zhu Q, Wang X, Yin Y, Kong X. Gut microbiota of newborn piglets with intrauterine growth restriction have lower diversity and different taxonomic abundances. *J Appl Microbiol.* 2019;127:354–69.
- He Q, Ren P, Kong X, Xu W, Tang H, Yin Y, Wang Y. Intrauterine growth restriction alters the metabolome of the serum and jejunum in piglets. *Mol Biosyst.* 2011;7:2147–55.
- D'Inca R, Che L, Thymann T, Sangild P, Le Huërou-Luron I. Intrauterine growth restriction reduces intestinal structure and modifies the response to colostrum in preterm and term piglets. *Livest Sci.* 2010;133:20–2.
- Wang J, Chen L, Li D, Yin Y, Wang X, Li P, Dangott LJ, Hu W, Wu G. Intrauterine growth restriction affects the proteomes of the small intestine, liver, and skeletal muscle in newborn pigs. *J Nutr.* 2008;138:60–6.
- Wang T, Huo YJ, Shi F, Xu RJ, Hutz RJ. Effects of intrauterine growth retardation on development of the gastrointestinal tract in neonatal pigs. *Neonatology.* 2005;88:66–72.
- Priante E, Verlatto G, Giordano G, Stocchero M, Visentin S, Mardegan V, Baraldi E. Intrauterine growth restriction: new insight from the metabolomic approach. *Metabolites.* 2019;9:267.
- Bahado-Singh RO, Yilmaz A, Bisgin H, Turkoglu O, Kumar P, Sherman E, Mrazik A, Odibo A, Graham SF. Artificial intelligence and the analysis of multi-platform metabolomics data for the detection of intrauterine growth restriction. *PLoS ONE.* 2019;14: e0214121. <https://doi.org/10.1371/journal.pone.0214121>.
- Sarr O, Yang K, Regnault TR (2012) In utero programming of later adiposity: the role of fetal growth restriction. *Journal of Pregnancy*
- Gondret F, Perruchot M-H, Tacher S, Bérard J, Bee G. Differential gene expressions in subcutaneous adipose tissue pointed to a delayed adipocytic differentiation in small pig fetuses compared to their heavier siblings. *Differentiation.* 2011;81:253–60.
- Attig L, Djiane J, Gertler A, Rampin O, Larcher T, Boukthir S, Anton P, Madec J-Y, Gourdou I, Abdennebi-Najar L. Study of hypothalamic leptin receptor expression in low-birth-weight piglets and effects of leptin supplementation on neonatal growth and development. *American J Physiol-Endocrinol Metab.* 2008;295:E1117–25.
- Gondret F, Lefaucheur L, Juin H, Louveau I, Lebreton B. Low birth weight is associated with enlarged muscle fiber area and impaired meat tenderness of the longissimus muscle in pigs. *J Anim Sci.* 2006;84:93–103.
- Ruggeri R, Bee G, Trevisi P, Ollagnier C. Intrauterine growth restriction defined by increased brain-to-liver weight ratio affects postnatal growth and protein efficiency in pigs. *Animal.* 2024;18: 101044.
- Kasper C, Schlegel P, Ruiz-Ascacibar I, Stoll P, Bee G. Accuracy of predicting chemical body composition of growing pigs using dual-energy X-ray absorptiometry. *Animal.* 2021;15: 100307.
- Takahashi S, Tomita J, Nishioka K, Hisada T, Nishijima M. Development of a prokaryotic universal primer for simultaneous analysis of Bacteria and Archaea using next-generation sequencing. *PLoS ONE.* 2014;9: e105592.
- R Core Team (2020) R: A language and environment for statistical computing
- Kneen M, Annegarn H. Algorithm for fitting XRF, SEM and PIXE X-ray spectra backgrounds. *Nucl Instrum Methods Phys Res, Sect B.* 1996;109:209–13.
- Liland KH, Almøy T, Mevik B-H. Optimal choice of baseline correction for multivariate calibration of spectra. *Appl Spectrosc.* 2010;64:1007–16.
- Wishart DS, Tzur D, Knox C, Eisner R, Guo AC, Young N, Cheng D, Jewell K, Arndt D, Sawhney S. HMDB: the human metabolome database. *Nucleic Acids Res.* 2007;35:D521–6.
- Dieterle F, Ross A, Schlotterbeck G, Senn H. Probabilistic quotient normalization as robust method to account for dilution of complex biological mixtures. Application in 1 H NMR metabolomics. *Anal Chem.* 2006;78(13):4281–90. <https://doi.org/10.1021/ac051632c>.
- Brugaletta G, De Cesare A, Laghi L, Manfreda G, Zampiga M, Oliveri C, Pérez-Calvo E, Litta G, Lolli S, Sirri F. A multi-omics approach to elucidate the mechanisms of action of a dietary muramidase administered to broiler chickens. *Sci Rep.* 2022;12:5559.
- Callahan BJ, McMurdie PJ, Rosen MJ, Han AW, Johnson AJA, Holmes SP. DADA2: high-resolution sample inference from Illumina amplicon data. *Nat Methods.* 2016;13:581–3.
- Quast C, Pruesse E, Yilmaz P, Gerken J, Schweer T, Yarza P, Peplies J, Glöckner FO. The SILVA ribosomal RNA gene database project: improved data processing and web-based tools. *Nucleic Acids Res.* 2012;41:D590–6.
- McMurdie PJ, Holmes S. phyloseq: an R package for reproducible interactive analysis and graphics of microbiome census data. *PLoS ONE.* 2013;8: e61217.
- Dixon P. VEGAN, a package of R functions for community ecology. *J Veg Sci.* 2003;14:927–30.
- Cao Y, Dong Q, Wang D, Zhang P, Liu Y, Niu C. microbiomeMarker: an R/Bioconductor package for microbiome marker identification and visualization. *Bioinformatics.* 2022;38:4027–9.
- Chao JM, de la Barca F, Chabrún TL, Roche O, Huetz N, Blanchet O, Legendre G, Simard G, Reynier P, Gascoin G. A metabolomic profiling of intra-uterine growth restriction in placenta and cord blood points to an impairment of lipid and energetic metabolism. *Biomedicines.* 2022;10(6):1411. <https://doi.org/10.3390/biomedicines10061411>.
- Hansen C, Hales J, Amdi C, Moustsen V. Intrauterine growth-restricted piglets defined by their head shape have impaired survival and growth during the suckling period. *Animal Prod Sci.* 2018;59:1056–62.
- Lynegaard J, Hansen C, Kristensen A, Amdi C. Body composition and organ development of intra-uterine growth restricted pigs at weaning. *Animal.* 2020;14:322–9.
- Alvarenga A, Chiarini-Garcia H, Cardeal P, Moreira L, Foxcroft G, Fontes D, Almeida F. Intra-uterine growth retardation affects birthweight and postnatal development in pigs, impairing muscle accretion, duodenal mucosa morphology and carcass traits. *Reprod Fertil Dev.* 2013;25:387–95.
- Xiong L, You J, Zhang W, Zhu Q, Blachier F, Yin Y, Kong X. Intrauterine growth restriction alters growth performance, plasma hormones, and small intestinal microbial communities in growing-finishing pigs. *J Animal Sci Biotechnol.* 2020;11:1–18. <https://doi.org/10.1186/s40104-020-00490-x>.
- Dwyer C, Fletcher J, Stickland N. Muscle cellularity and postnatal growth in the pig. *J Anim Sci.* 1993;71:3339–43.
- Gondret F, Lefaucheur L, Louveau I, Lebreton B, Pichodo X, Le Cozler Y. Influence of piglet birth weight on postnatal growth performance, tissue lipogenic capacity and muscle histological traits at market weight. *Livest Prod Sci.* 2005;93:137–46.
- Rontogianni A, Dontas IA, Halazonetis D, Tosios K, Lelovas P, Venetsanou K, Galanos A, Tsolakis AI. Intrauterine growth restriction affects bone mineral density of the mandible and the condyle in growing rats. *J Musculoskelet Neuronal Interact.* 2022;22:93.

43. Zhang J, Yan E, Zhang L, Wang T, Wang C. Curcumin reduces oxidative stress and fat deposition in longissimus dorsi muscle of intrauterine growth-retarded finishing pigs. *Anim Sci J*. 2022;93: e13741.
44. Latorre M, Medel P, Fuentetaja A, Lázaro R, Mateos G. Effect of gender, terminal sire line and age at slaughter on performance, carcass characteristics and meat quality of heavy pigs. *Anim Sci*. 2003;77:33–45.
45. Suárez-Belloch J, Guada J, Latorre M. Effects of sex and dietary lysine on performances and serum and meat traits in finisher pigs. *Animal*. 2015;9:1731–9.
46. Yang Y, Liu Y, Liu J, Wang H, Guo Y, Du M, Cai C, Zhao Y, Lu C, Guo X. Composition of the fecal microbiota of piglets at various growth stages. *Front Veterinary Sci*. 2021;8: 661671.
47. Gaukroger CH, Stewart CJ, Edwards SA, Walshaw J, Adams IP, Kyriazakis I. Changes in faecal microbiota profiles associated with performance and birthweight of piglets. *Front Microbiol*. 2020;11:917.
48. Kim HB, Borewicz K, White BA, Singer RS, Sreevatsan S, Tu ZJ, Isaacson RE. Longitudinal investigation of the age-related bacterial diversity in the feces of commercial pigs. *Vet Microbiol*. 2011;153:124–33.
49. Nowland T, Kirkwood R, Pluske J. Can early-life establishment of the piglet intestinal microbiota influence production outcomes? *Animal*. 2022;16: 100368.
50. Lan Q, Lian Y, Peng P, Yang L, Zhao H, Huang P, Ma H, Wei H, Yin Y, Liu M. Association of gut microbiota and SCFAs with finishing weight of Dian-nan small ear pigs. *Front Microbiol*. 2023;14:1117965.
51. Farmer C, Edwards S. Improving the performance of neonatal piglets. *Animal*. 2022;16: 100350.
52. Le Sciellour M, Labussière E, Zemb O, Renaudeau D. Effect of dietary fiber content on nutrient digestibility and fecal microbiota composition in growing-finishing pigs. *PLoS ONE*. 2018;13: e0206159.
53. Dowarah R, Verma A, Agarwal N. The use of *Lactobacillus* as an alternative of antibiotic growth promoters in pigs: a review. *Animal Nutr*. 2017;3:1–6.
54. Zhang L, Wu W, Lee Y-K, Xie J, Zhang H. Spatial heterogeneity and co-occurrence of mucosal and luminal microbiome across swine intestinal tract. *Front Microbiol*. 2018;9:48.
55. Lin G, Liu C, Feng C, Fan Z, Dai Z, Lai C, Li Z, Wu G, Wang J. Metabolomic analysis reveals differences in umbilical vein plasma metabolites between normal and growth-restricted fetal pigs during late gestation. *J Nutr*. 2012;142:990–8.
56. Suryawan A, Jeyapalan AS, Orellana RA, Wilson FA, Nguyen HV, Davis TA. Leucine stimulates protein synthesis in skeletal muscle of neonatal pigs by enhancing mTORC1 activation. *American J Physiol-Endocrinol Metabol*. 2008;295:E868–75.
57. Escobar J, Frank JW, Suryawan A, Nguyen HV, Kimball SR, Jefferson LS, Davis TA. Physiological rise in plasma leucine stimulates muscle protein synthesis in neonatal pigs by enhancing translation initiation factor activation. *American J Physiol-Endocrinol Metabol*. 2005;288:E914–21.
58. Yin Y, Yao K, Liu Z, Gong M, Ruan Z, Deng D, Tan B, Liu Z, Wu G. Supplementing L-leucine to a low-protein diet increases tissue protein synthesis in weanling pigs. *Amino Acids*. 2010;39:1477–86.
59. Wixey JA, Lee KM, Miller SM, Goasdoue K, Colditz PB, Tracey Bjorkman S, Chand KK. Neuropathology in intrauterine growth restricted newborn piglets is associated with glial activation and proinflammatory status in the brain. *J Neuroinflammation*. 2019;16:1–13.
60. Wang X, Liu Y, Li S, Pi D, Zhu H, Hou Y, Shi H, Leng W. Asparagine attenuates intestinal injury, improves energy status and inhibits AMP-activated protein kinase signalling pathways in weaned piglets challenged with *Escherichia coli* lipopolysaccharide. *Br J Nutr*. 2015;114:553–65.
61. Guoyao W. Functional amino acids in nutrition and health. *Amino Acids*. 2013;45(3):407–11. <https://doi.org/10.1007/s00726-013-1500-6>.
62. Chen S, Liu Y, Wang X, Wang H, Li S, Shi H, Zhu H, Zhang J, Pi D. Hu C-AA: asparagine improves intestinal integrity, inhibits TLR4 and NOD signaling, and differently regulates p38 and ERK1/2 signaling in weanling piglets after LPS challenge. *Innate Immun*. 2016;22:577–87.
63. Wu H, Liu Y, Pi D, Leng W, Zhu H, Hou Y, Li S, Shi H, Wang X. Asparagine attenuates hepatic injury caused by lipopolysaccharide in weaned piglets associated with modulation of Toll-like receptor 4 and nucleotide-binding oligomerisation domain protein signalling and their negative regulators. *Br J Nutr*. 2015;114:189–201.

Publisher's Note

Springer Nature remains neutral with regard to jurisdictional claims in published maps and institutional affiliations.